IEEE Access
Multidisciplinary ⋮ Rapid Review ⋮ Open Access Journal

Received December 17, 2019, accepted December 27, 2019, date of publication January 7, 2020, date of current version January 15, 2020.

Digital Object Identifier 10.1109/ACCESS.2020.2964319

RVFL-LQP: RVFL-Based Link Quality Prediction of Wireless Sensor Networks in Smart Grid

XUE XUE[1], WEI SUN[1], (Member, IEEE), JIANPING WANG[1], QIYUE LI[1], (Member, IEEE), GUOJUN LUO[1], AND KEPING YU[2,3], (Member, IEEE)

[1]School of Electrical Engineering and Automation, Hefei University of Technology, Hefei 230009, China
[2]Global Information and Telecommunication Institute, Waseda University, Tokyo 169-8050, Japan
[3]Shenzhen Boyi Technology Co., Ltd., Shenzhen 518125, China

Corresponding author: Wei Sun (wsun@hfut.edu.cn)

This work was supported in part by the National Natural Science Foundation of China under Grant 51877060, in part by the Fundamental Research Funds for the Central Universities of China under Grant PA2019GDQT0006 and Grant JZ2018HGTB0253, and in part by the Science and Technology Project of State Grid Corporation of China (Research and Application of Key Technologies for Operation and Maintenance of Smart Substation Based on the Fusion of Heterogeneous Network and Data).

ABSTRACT In the application of wireless sensor networks (WSNs) to smart grid, real-time and accurate wireless link quality prediction (LQP) is important to determine which link is reliable enough to undertake the communication task. However, the existing LQP methods are neither suitable to describe the dynamic stochastic features of link quality nor to ensure the validity of prediction results. In this paper, a random-vector-functional-link-based LQP (RVFL-LQP) algorithm is proposed. The algorithm selects the signal-to-noise ratio (SNR) as the link quality metric and decomposes the raw SNR sequence into the time-varying sequence and the stochastic sequence according to the analysis of wireless link characteristics. Then, the RVFL network is used to establish the prediction model of the time-varying sequence and the variance of the stochastic sequence. Lastly, the probability-guaranteed interval boundary of SNR is predicted, and the validity and practicability of prediction results are evaluated by comparative experiments and real-world application, respectively.

INDEX TERMS Wireless sensor networks, link quality prediction, RVFL network, probability-guaranteed interval boundary.

I. INTRODUCTION

The increasing demand for the reliability of the electricity supply promotes the modernization of the power grid system, which is called the smart grid. The smart grid is an integrated cyber-physical system composed by power grid and communication network to support bi-directional flows of electricity and information for more effectively coordinate the global electrical energy among the generators and consumptions [1]–[2]. Nevertheless, how to realize the ubiquitous communication over a huge number of geographically distributed power grid devices in the wide-ranging area is a challenge.

Due to the high cost of install and maintenance, the poor scalability features, the traditional wired network technologies are not suitable for the communication of widely distributed and large-scale power grid devices [2]. On the other hand, wireless sensor networks (WSNs) had attracted extensive attention because of their features of low cost, ease of deployment, and versatility [3]–[5]. In 2011, the ''Development Framework and Roadmap of Smart Grid'' by NIST listed the ZigBee protocol (a specification of WSNs) as one of the recommended communication standards for smart grid. In the meanwhile, IEEE 802.15.4g, the lower layers protocols of ZigBee, is released, which is exclusively used in utility smart-grid network and capable of supporting large and geographically diverse networks [6]. The standards specialized for smart grid further facilitates its applications, including power fraud detection, transmission line monitoring, fault diagnostics, load control, and distribution automation application [7]–[11].

Although the WSNs have many advantages for the applications in smart grid, there still exist some issues. One of them is to satisfy the reliability requirements of smart grid. Commonly, the wireless signal is stochastic changing caused by multipath interference, background noise, and shadow fading, etc., which leads to the time-varying fluctuation of the wireless link quality. This dynamically stochastic feature

The associate editor coordinating the review of this manuscript and approving it for publication was Giovanni Pau.

This work is licensed under a Creative Commons Attribution 4.0 License. For more information, see http://creativecommons.org/licenses/by/4.0/

affects the reliability of the wireless link. Although the protocol of WSNs improves reliability through the retransmission mechanism, the increased delay leads to a degradation of overall network efficiency. Because there are a lot of redundancy wireless links in the mesh-sharp topology of WSNs, when the quality of one link degrades significantly, the WSNs node could choose a high-quality link for transmitting. Therefore, predicting the link quality of WSNs helps WSNs to make a routing-path decision and avoid packet loss in advance.

In literature, there are a lot of studies focused on the link quality prediction (LQP). Shu *et al.* [12] propose an LQP mechanism which based on dynamic Bayesian networks to achieve better accuracy and robustness. Zhou *et al.* [13] design a compressive-sensing-based LQP to aid the link update in routing protocols. Qin *et al.* [14] propose an augmented Kalman-filter-based LQP, the results of experiments show that LQP performance is significantly improved in comparison with conventional Kalman-filter-based LQP. Cerar *et al.* [15] systematically study the performance of machine learning-based LQP. The LQP methods proposed in [12]–[15] provide an accurate numerical prediction. However, they all use the deterministic numerical prediction results to describe the stochastic features of link quality. Even the LQP results meet the requirements of reliability, due to the stochastic fluctuation, the actual link quality may lower than the requirements.

Motivated by more appropriately describing and predicting the stochastic wireless link quality for smart grid application, we carried out RVFL-Based link quality prediction by probability-guaranteed prediction results. In this paper, we first analyze the characteristics of the SNR that is chosen as the wireless link quality metric. Based on the analysis, we decompose the SNR sequence into the time-varying sequence and the stochastic sequence. Then we construct an RVFL model to innovatively predict the time-varying sequence and the variance of the stochastic sequence. From the perspective of statistical analysis, probability-guaranteed prediction of the interval boundary of link quality is carried out, which helps WSNs node to judge which link meets the reliability requirements, and to select a more reliable wireless link path among several available links.

The main novelty and contributions of our study are listed as follows.

1. According to the theoretical analysis based on the log-normal path-loss model, the link quality metric (SNR) is creatively decomposed into the time-varying part and the stochastic part.

2. A novel RVFL model is proposed to predict two parts of the link quality metric (SNR), which vary nonlinearly according to the change of the surrounding environment, more accurately.

3. The probability-guaranteed interval boundary, which more suitable for reflecting the stochastic fluctuation of the dynamic radio link, is predicted.

4. The RVFL-LQP algorithm is verified by real-world experiments.

The rest of the paper is organized as follows. Section II summarizes some related work. Then, section III analyzes the network topology and the characteristics of the link quality metric. The RVFL-LQP algorithm is elaborated in section IV. Section V presents all the experiments in different conditions. In section VI, the application example is illuminated. Finally, we present the conclusions of this study in Section VII.

II. RELATED WORK

A. LINK QUALITY METRICS AND RELATED METHODS

To rapidly estimate or predict the state of the wireless link, a lot of methods for LQP are proposed. According to the metrics they adopted, the existing methods can be classified into three categories, including *physical metrics based, logical metrics based, and hybrid metrics based* [16].

1) PHYSICAL METRICS BASED LQP

The hardware of WSNs node, for example, the TI CC2530, a widely used low power radio chip, provides the Received Signal Strength Indication (RSSI) and the Link-Quality Indication (LQI) after successful transmission. Furthermore, the environmental noise can be measured by CC2530 while there is no transmission in progress, which helps to get the Signal-to-Noise Ratio (SNR). Since the physical metrics are easy to be obtained, there are many Physical Metrics based LQP methods. Reijers *et al.* [17] propose a method that uses RSSI to predict the link quality. Chen et al. [18] use RSSI calibration to improve the quality of measurements, but this method may introduce higher computational complexity, which makes it unsuitable for low-cost WSNs. However, when LQI is very high, it can be used to identify high-quality links [19]. Otherwise, it is difficult to determine whether the link quality is good or not by LQI. Although it is more accurate to predict the link quality by mean of LQI which can be calculated by a certain number of packets within a window, this approach realized at the expense of the reducing sensitivity to the change of link quality, and the length of the calculating window size is difficult to determine. Senel *et al.* [20] propose an LQP method based on a Kalman filter. They filter the RSSI and remove the noise floor in order to collect the smooth value of SNR. However, this approach is very complex and does not provide a sufficiently detailed description of link quality.

2) LOGICAL METRICS BASED LQP

The logical metrics are the statistical results of the packet reception/retransmission rate from the higher layer of WSNs protocol, i.e., the application layer, to assess the link quality. The commonly used logical metrics include Packet Reception Rate (PRR), Required Number of Packets (RNP), or Expected Transmission Count (ETX). They can directly reflect the reliability performance of higher layer without relying on any hardware. In comparison to physical metrics, LQPs based

on logical metrics have to execute frequent packet transmission to obtain up-to-date metric values. Woo *et al.* [21] adopt PRR as the metric and use the WMEWMA estimator to predict the link quality among nodes. Although PRR can be obtained easily, a lot of historical data have to be recorded to compute accurate PRR. Furthermore, the wireless link has characters of unstable and asymmetrical. However, the PRR cannot evaluate those characters of link quality [22]. Moinzadeh et al. [23] present an RNP-based evaluation method, in which, the potential distribution loss problems are taken into account. This method is executed on the sender. It counts the number of packets sent by the sender before the packet is successfully received. Moreover, RNP cannot accurately evaluate links due to link asymmetry. Wang *et al.* [24] study a passive-monitoring-mode-based LQP method, in which, the EXT has been selected as the metric to predict link quality. However, the method fails in overloaded networks. In addition, Couto *et al.* [25] propose a routing protocol based on the ETX metric to choose the high-throughput paths, but ETX cannot reflect fast-changing links timely.

3) HYBRID METRICS BASED LQP

The combination of different metric parameters could be deemed as hybrid metrics. Some hybrid based LQP methods have been proposed in order to obtain more comprehensive link information. In literature, Boano *et al.* [26] adopt the geometrical graph theory to propose the triangle metric, which geometrically combines the information of PRR, LQI, and SNR into a robust estimator, in order to obtain a rapid and trustworthy assessment of the link quality. Baccour *et al.* [27] introduce the Fuzzy Link Quality Estimation algorithm (F-LQE), which uses fuzzy logic to combine four link properties (the link stability, link asymmetry, channel quality, and packet delivery). However, in the modeling process, the membership function not only needs to be artificially defined but also needs to be changed as the scene changes. Jayasri and Hemalatha [28] consider all the four link quality indexes (PRR, ALQI, ASNR, and SA), and propose the enhanced link quality estimation technique (ELQET). Based on ELQET, the link quality can be classified into good or poor categories, but the link quality has high generalization under different environments. Liu *et al.* [29] present a link quality evaluation approach based on 4-bits, which combines the information of the network layer, data link layer, and physical layer. This method could significantly improve the accuracy and timeliness of link estimation.

All the above LQP methods could provide numerical predictions with different accuracy. However, the strong stochastic feature of the wireless link is not considered. Even the predictions are executed correctly, the prediction results may fluctuate up and down around the actual link quality. The foundational reason is that they use the deterministic number to describe the link quality with the stochastic feature. This motivates us introducing probability-guaranteed prediction of the interval boundary to more correctly describe the stochastic feature of wireless link quality. It's worth noting that, although the Kalman-filter-based prediction can provide the boundary prediction, it based on an accurate linear model. For the prediction of the nonlinear model, linearization is required, and the linearization introduces errors.

TABLE 1. The requirements of smart grid applications.

Application	Reliability requirements
Demand Response Management	99.0-99.99%
Distribution Automation	99.0-99.99%
Distributed Energy Resources and Storage	99.0-99.99%
Overhead Transmission Line Monitoring	95.0-99.99%
Asset Management	99.0-99.99%
Outage Management	95.0-99.99%
Substation Automation	99.0-99.99%
Distribution Management	99.0-99.99%

B. SELECTION OF THE LQP METRIC FOR SMART GRID

In the application of wireless sensor networks to smart grid, the main challenge lies in how to satisfy the reliability requirements for diverse smart grid applications.

Table 1 summarizes that different smart grid applications have each specific reliability requirements [30]. The requirements are presented in the form of communication success rate, which could be deemed as the PRR for WSNs. In general, PRR is the statistical results which statistically computed over a period of time. WSNs nodes have to record a lot of historical data to compute the accurate PRR. However, the PRR only reflects the average link quality over this period of time, it cannot reflect the dynamic change of link quality in a piece of time.

On the other hand, based on the modulation mode (for example, O-QPSK) that WSNs adopted, the mapping function between SNR and PRR of radio link quality [31] is expressed by (1).

$$\gamma_{PRR} = \varphi(\gamma_d) = \left(1 - Q\left(\sqrt{2 \times 10^{\frac{\gamma_d}{10}} \frac{B_N}{R}}\right)\right)^{8l} \tag{1}$$

where γ_d is the SNR value, γ_{PRR} is the PRR value (It's worth noting that this PRR is not the statistical results introduced above, it is the computed PRR from the mapping function $\varphi(\cdot)$), B_N is the noise bandwidth associated with the wireless transceiver in kHz, l is the packet length, $Q(\cdot)$ is a right tail function of the standard normal distribution, and R is the data transmission rate in kbps.

Thanks to the mapping function between SNR and PRR, the reliability of WSNs communication of smart grid also could be characterized by SNR. Moreover, SNR can be

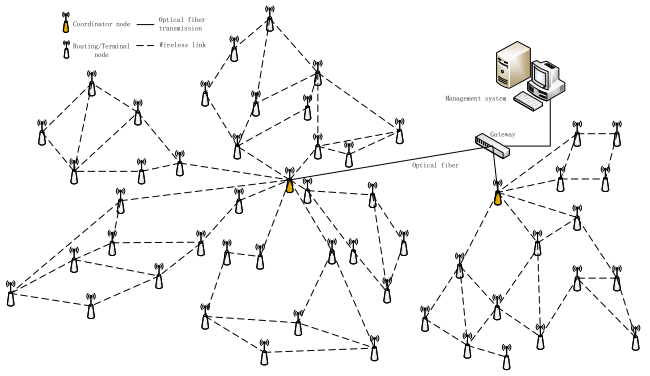

FIGURE 1. Topology of WSNs in smart grid.

directly obtained from hardware and immediately reflect the fast change of the received signal strength and overall noise. Then, by using the mapping function to obtain PRR, the drawbacks of insensitive to dynamical change of link quality by statistical PRR is avoided. Therefore, SNR is chosen as the link quality metric in this paper.

III. WSNs IN SMART GRID

In this section, we first give the topology of WSNs that considered in smart grid applications. Then, the characteristics of the link quality metric are theoretically analyzed.

A. TOPOLOGY OF WSNs IN SMART GRID

The network topology composing wired and wireless networks to form WSNs communication in smart grid is presented in Fig.1. In this topology, the optical fiber communication is used to expand the distance of the WSNs. In the meanwhile, the WSNs covering the branches and terminal equipment is used to improve the range of point-to-point optical fiber. The coordinator node connects to the gateway via optical fiber, and finally links to the smart grid management system.

The WSNs in Fig.1 are a mesh-type complex network [32], [33]. When a WSNs node could not directly communicate with the coordinator node, the multi-hop relay mechanism is adopted. Although there exist two or three-node motif, thanks to the routing protocol of WSN, each node only has to concerns the reliability of the link between itself and its next hop neighbor on the routing path. In other words, when a node has more than one routing path to upload data, it can predict the quality of the links with its neighbors based on the historical and real-time information, and then choose a neighbor with more reliable link to forward data. In this manner, link quality prediction is essential to estimate the routing path. Therefore, in this paper, we only consider the relationship between a node and its neighbor nodes in the network, because all nodes could adopt the same scheme.

B. THE THEORETICAL CHARACTER OF SNR

There are several radio propagation models for analyzing the radio link in WSNs, including ground bidirectional reflectance model, free-space model, and log-normal path-loss model. Since the log-normal path-loss model can reflect almost all kinds of environment and disturbance factors under different variables, and is suitable for both high-density building and low-density building areas, it is commonly adopted as a general propagation model for WSNs in smart grid applications [34]–[37]. The log-normal path-loss model describes the relationship between the signal strength of received electromagnetic wave and transmission paths. By taking the background noise into account, the SNR (in dBm) of the communication link [37], [38] is given by:

$$\gamma_d = P_{tx} - PL\,(d_0) - 10\eta log_{10}(\frac{d}{d_0}) - X_\sigma - P_n \qquad (2)$$

where γ_d is the SNR of the received signal when the distance between the receiver and transmitter is d, P_{tx} denotes the output power of the transmitter in dBm, and $PL\,(d_0)$ is the power decay after transmitting d_0 meters, d_0 is the reference distance which is commonly chosen 1m. η is the path-loss exponent, which depends on the surrounding environment. X_σ is the influence of multipath effect on the received signal, and it is expressed as a zero mean Gaussian random process with standard deviation σ_x,which can be represented as $X_\sigma \sim N(0, \sigma_x^2)$.

Meanwhile, P_n represents the background noise power in dBm, it can be approximated as the Gaussian noise, which subjects to a Gaussian distribution with a time-varying mean of $\overline{P_n}$ and variance of σ_n^2, i.e., $P_n \sim N(\overline{P_n}, \sigma_n^2)$.We define the variable X_n as (3).

$$X_n = P_n - \overline{P_n} \qquad (3)$$

It's known that $X_n \sim N(0, \sigma_n^2)$, then substitute (3) into (2), we can get (4).

$$\gamma_d = P_{tx} - PL\,(d_0) - 10\eta log_{10}(\frac{d}{d_0}) - \overline{P_n} - (X_\sigma + X_n) \qquad (4)$$

From (4), the SNR consists of two parts: (1) the time-varying part, $P_{tx} - PL\,(d_0) - 10\eta log_{10}(d/d_0) - \overline{P_n}$, and (2) the stochastic part, $X_\sigma + X_n$.The mean of background noise, the path-loss exponent, the transmission power, and the distance may change over time in communication, they reflect the time-varying and nonlinear characteristics of the signal in space. Meanwhile, the stochastic part is the combination of two Gaussian random variables, whose mean is 0 and variance σ^2 is expressed as (5).

$$\sigma^2 = \sigma_x^2 + \sigma_n^2 \qquad (5)$$

According to the theoretical analysis above, it is clear that the link quality metric, SNR, is composed of two parts with quite different features. Therefore, in the link prediction, we focus on improving prediction methods for dealing with these characteristics.

IV. RVFL-LQP ALGORITHM

The theoretical analysis results motivate us to decompose the SNR signal into the time-varying part and the stochastic

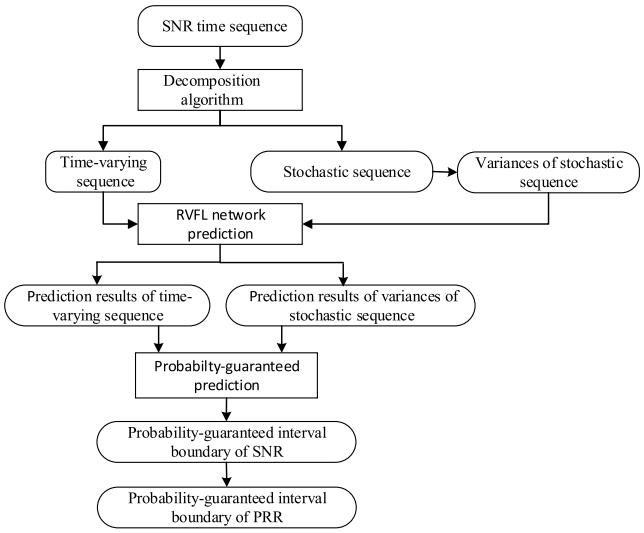

FIGURE 2. RVFL-LQP algorithm structure.

part. In this section, we propose the RVFL-LQP algorithm to predict the SNR time sequence. Fig.2 shows the RVFL-LQP algorithm, which consists of signal decomposition, RVFL network prediction, and probability-guaranteed prediction.

Based on the analysis of wireless communication links, the SNR is a kind of time sequence with time-varying and stochastic characteristics. We first decompose the raw SNR time sequence into the time-varying sequence and the stochastic sequence. Then we calculate the variances of the stochastic sequence to better describe the stochastic characteristics. Consequently, the RVFL network is used to predict the time-varying sequence and the variances of the stochastic sequence, respectively. Lastly, we obtain the probability-guaranteed interval boundary of PRR as the prediction results to indicate the link reliability for smart grid application.

A. DECOMPOSITION ALGORITHM OF WIRELESS LINK QUALITY

To decompose the time-varying part and stochastic part, we introduce the moving-average filter to pre-process raw SNR sequence for more convenient and effective.

Suppose the WSNs node recorded raw SNR sequence, which is noted by $R(L) = \{r_1, r_2, \cdots r_L\}$. Through the moving-average filter, the time-varying sequence part, noted by $RT(L) = \{rt_1, rt_2, \cdots rt_L\}$, is expressed as:

$$rt_k = \begin{cases} \dfrac{r_1 + r_2 + \cdots + r_k}{k}, & k = 1, 2, \cdots, W_1 - 1 \\ \dfrac{r_{k-W_1+1} + r_{k-W_1+2} + \cdots + r_k}{W_1}, & k = W_1, W_1 + 1, \cdots, L \end{cases} \tag{6}$$

where W_1 ($W_1 < L$) is the moving window size to calculate the time-varying sequence.

And the other decomposed part, the stochastic sequence part, noted by $RS(L) = \{rs_1, rs_2, \cdots rs_L\}$ shows as:

$$rs_k = r_k - rt_k, \quad k = 1, 2, \cdots, L \tag{7}$$

In addition, when we choose the suitable moving window size, it may take a short time to send the packets within the window. In the meanwhile, as shown in equation (4), $X_\sigma + X_n$ is the stochastic process, X_σ is the influence of multipath effect on the received signal, X_n is affected by the background noise of the environment. In a short time, we assume the surrounding environment does not change tremendously, we can approximate the multipath effect and background noise as the stationary process. So we approximate $RS(L)$ as a stationary stochastic process as well. Then we can obtain straightforwardly the variances of the stochastic sequence, noted by $RV(L) = \{rv_1, rv_2, \cdots, rv_L\}$ shows as:

$$rv_k = \begin{cases} \dfrac{1}{k}\sum_{i=1}^{k}\left(rs_i - \dfrac{rs_1 + rs_2 + \cdots + rs_k}{k}\right)^2, \\ \qquad k = 1, 2, \cdots W_2 - 1 \\ \dfrac{1}{W_2}\sum_{i=1}^{W_2} \\ \left(rs_{k-W_2+i} - \dfrac{rs_{k-W_2+1} + rs_{k-W_2+2} + \cdots + rs_k}{W_2}\right)^2, \\ \qquad k = W_2, W_2 + 1, \cdots, L \end{cases} \tag{8}$$

where W_2 ($W_2 < L$) is the moving window size to calculate the variances sequence.

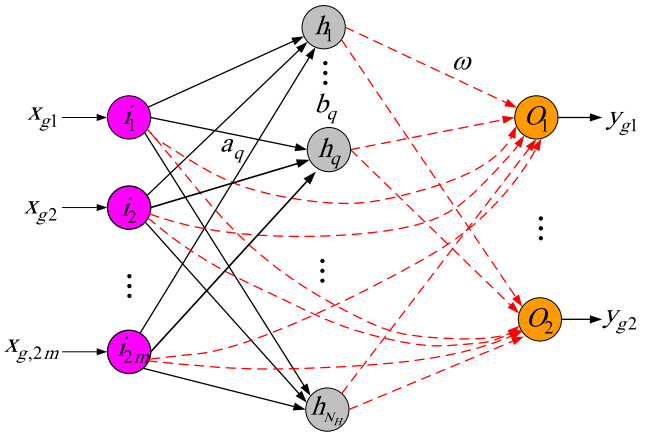

FIGURE 3. RVFL network model structure.

B. RVFL NETWORK PREDICTION MODEL

Both the time-varying sequence and the variances of the stochastic sequence vary nonlinearly according to the change of the surrounding environment. To address the problems of predicting SNR, in this section, we adopt the non-iterative RVFL neural network to achieve the fast and accurate prediction for two parts of the decomposed SNR sequence.

The RVFL network is a special case of single hidden layer feed-forward neural networks, and it appears faster compared with traditional neural networks which are iterative learning. Furthermore, the network presents more effective relative to non-iterative networks which without the direct input-output links.

Fig. 3 depicts the architecture of the RVFL model which we adopt. In this model, we consider the time-varying sequence $RT(m) = \{rt_j, rt_{j+1}, rt_{j+2}, \cdots rt_{j+m-1}\}$,

and the variances of the stochastic sequence $RV(m) = \{rv_j, rv_{j+1}, rv_{j+2}, \cdots rv_{j+m-1}\}$ as the input data. The output data are the predicted rt_{j+m} and $rv_{j+m}(j+m \leq L)$. For convenience, all input data for N samples is represented by $x_{gn}(g = 1, 2, \cdots, N; n = 1, 2, \cdots, 2m)$, all output data for N samples is represented by $y_{gh}(g = 1, 2, \cdots, N; h = 1, 2)$, i.e., the number of input layer nodes is $N_I = 2 \cdot m$, the number of output layer nodes is $N_O = 2$, respectively. Then after many experiments, we choose the optimal number of hidden layer nodes $N_H = 33$.

Furthermore, the RVFL network uses direct links to connect input layer nodes with output layer nodes. Then an RVFL network with N_H hidden layer nodes can be formulated as:

$$H\omega = Y \tag{9}$$

where H is a complicated matrix combining input data and outputs from the hidden layer nodes, ω is an output weight vector drawn by dashed arrows, and Y is an output matrix. Then H and ω are shown as:

$$\begin{aligned} H &= [H_1 H_2] \\ H_1 &= \begin{bmatrix} x_{11} & \cdots & x_{1,2m} \\ \vdots & \ddots & \vdots \\ x_{N1} & \cdots & x_{N,2m} \end{bmatrix} \\ H_2 &= \begin{bmatrix} G(a_1 \cdot x_1 + b_1) & \cdots & G(a_{N_H} \cdot x_1 + b_{N_H}) \\ \vdots & \ddots & \vdots \\ G(a_1 \cdot x_N + b_1) & \cdots & G(a_{N_H} \cdot x_N + b_{N_H}) \end{bmatrix} \end{aligned} \tag{10}$$

$$\omega = \begin{bmatrix} \omega_1^T \\ \vdots \\ \omega_{(2m+N_H)}^T \end{bmatrix} \tag{11}$$

where $x_g = \left[x_{g1}, x_{g2}, \cdots, x_{g,2m}\right]^T (g = 1, 2, \cdots, N)$, $G(\cdot)$ is the activation function, $a_q = \left[a_{q1}, a_{q2}, \cdots, a_{q,2m}\right](q = 1, 2, \cdots, N_H)$ is the input weight of the q-th hidden layer node drawn by solid arrows, and $b_q(q = 1, 2, \cdots, N_H)$ is the bias of the q-th hidden layer node. To reduce the iterative adjustment time, the random values of all input weights and biases are uniformly distributed in the interval [−1,1] and [0,1].

We directly calculate the output weights ω by the Moore-Penrose pseudo-inverse, which are shown in (12).

$$\omega = H^{\dagger} Y = (H^T H)^{-1} H^T Y \tag{12}$$

where the symbol † denotes the Moore-Penrose pseudo-inverse.

In summary, the process of training the RVFL network is as follows:

(1) Distribute random values to input weight a_q and bias b_q, respectively.
(2) Obtain the complicated matrix H, where $G(x) = \frac{1}{1+e^{-x}}$, and the input data is the training data.
(3) Apply least square estimation to calculate the output weights ω, where Y is the training target.

Then combining the obtained a_q, b_q, ω with the test data, we could calculate the prediction results for the test data by (13).

$$\hat{Y} = \hat{H}\omega \tag{13}$$

where the input data contained in $\hat{H}$ is the test data, and $\hat{Y}$ is the prediction results for test data.

C. PROBABILITY-GUARANTEED INTERVAL PREDICTION OF LINK RELIABILITY

In this paper, the output data, rt_{j+m} and rv_{j+m} are predictions of the $RT(m)$ and $RV(m)$, respectively. Meanwhile, rt_{j+m} could be deemed as the mean of the predicted SNR value r_{j+m}, and rv_{j+m} could be deemed as the variance of the predicted SNR value r_{j+m}. According to the analysis of (4), the SNR can be regarded as a Gaussian distribution with mean rt_{j+m} and variance rv_{j+m}.

Due to the SNR are stochastic, we introduce the probability-guaranteed interval to express the prediction value of SNR. To satisfy the requirements of the reliability for smart grid applications, the probability-guaranteed prediction of interval boundary (lower boundary) on the SNR can be expressed as:

$$\left[rt_{j+m} - z_\alpha \cdot \sqrt{rv_{j+m}}, +\infty\right) \tag{14}$$

where α represents the probability-guaranteed level and z_α is the α-th quantile of the Normal distribution.

The relationship between SNR and PRR expressed according to equation (1), the probability-guaranteed prediction of interval boundary (lower boundary) on the PRR can be expressed as:

$$\left[\varphi\left(rt_{j+m} - z_\alpha \cdot \sqrt{rv_{j+m}}\right), +\infty\right) \tag{15}$$

where the function $\varphi(\cdot)$ is expressed in equation (1).

V. EXPERIMENTAL ANALYSIS

In this section, we conduct several experiments to evaluate the proposed RVFL-LQP algorithm on WSNs testbed in a power substation. The experimental WSNs include eleven CC2530 transceiver nodes and random obstructions between WSNs nodes.

As shown in Fig.1, the WSNs of smart grid may have a lot of nodes. Those distant nodes have no impact on the current wireless link. In our prediction algorithm, we only consider the point-to-point radio link quality. So, ten neighbor nodes around one are dense enough to represent a congested radio channel as a part of WSNs. In the experiment, three WSNs links are selected, their spacing distance are 10m, 50m, and 90m, respectively.

All nodes work on the 2.4GHz band with a maximum data transmission rate of 250 kbps. The length of each packet is 20 bytes. On those links, nodes send packets from one to another every 300ms. Then we collect the received signal strength and the measured background noise to calculate the SNR as shown in the (4). Then, prediction algorithms are carried out.

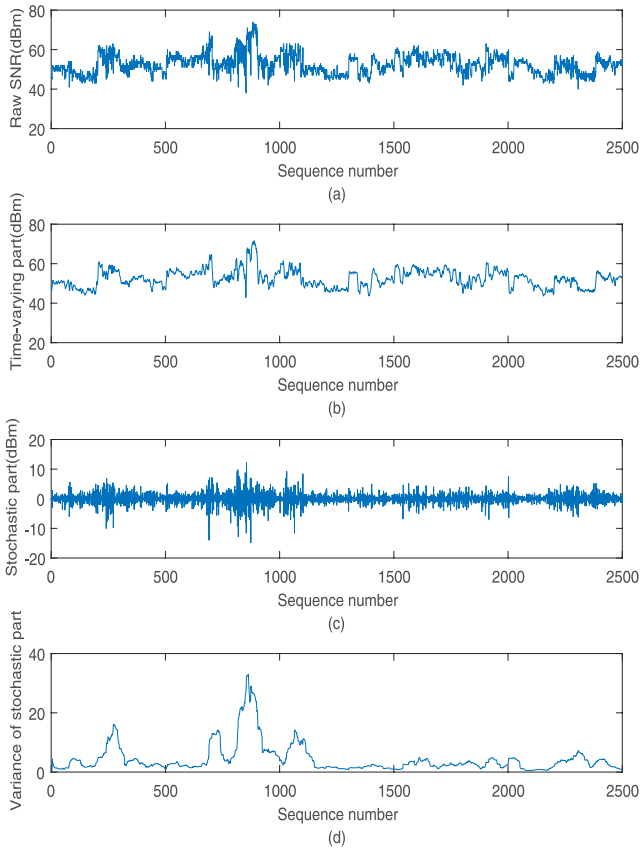

FIGURE 4. In the case of 10m spacing distance: (a) raw SNR sequence, (b) time-varying sequence, (c) stochastic sequence, and (d) variances of stochastic sequence.

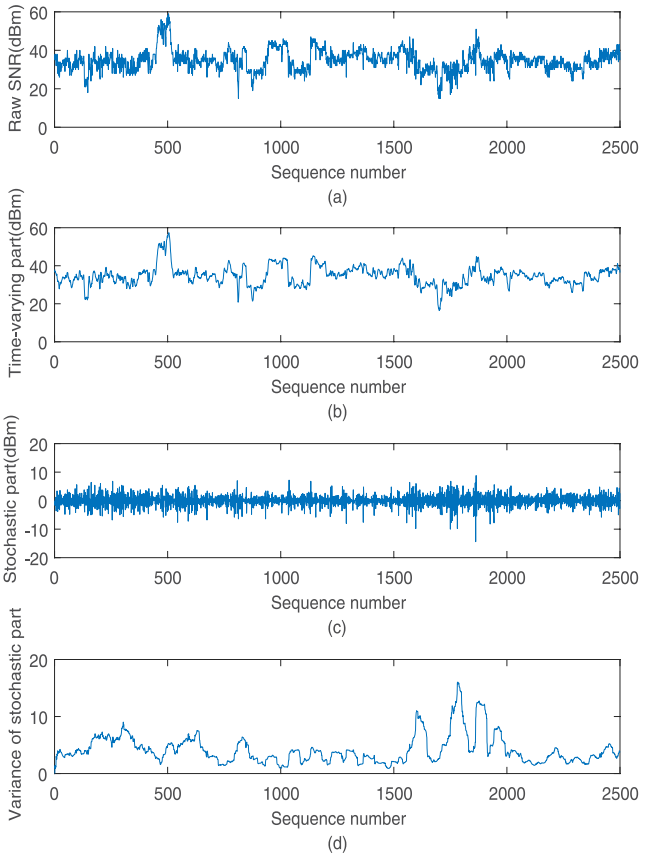

FIGURE 5. In the case of 50m spacing distance: (a) raw SNR sequence, (b) time-varying sequence, (c) stochastic sequence, and (d) variances of stochastic sequence.

A. DECOMPOSITION OF SNR

Firstly, all SNR sequence are collected and decomposed. The decomposed SNR sequence for three WSNs links (spacing distance are 10m, 50m, and 90m, respectively) is recorded to train the proposed RVFL algorithm. The decomposition process is depicted in Fig.4, Fig.5, and Fig.6.

From the collected raw SNR sequence of three different cases in Fig.4(a), Fig.5(a) and Fig.6(a), as the spacing distance increases, the average value of SNR decreases gradually. By the proposed decomposition method, the corresponding time-varying parts are extracted ($W_1 = 10$) (see Fig.4(b), Fig.5(b) and Fig.6(b)). And the stochastic sequence varies randomly have a mean of nearly zero (see Fig.4(c), Fig.5(c) and Fig.6(c)). In addition, the variances of the stochastic sequence are calculated as shown in Fig.4(d), Fig.5(d) and Fig.6(d) ($W_2 = 30$). These results verify the analysis of Section III B and Section IV A. Then, the decomposed results are used to train the output weight coefficients ω for the three radio links.

B. PREDICTION RESULTS

As the original data sequence decomposed into two individual sequences here, we use the non-iterative RVFL network to predict each individual part. Based on the trained output weight coefficients ω, we predict the lower boundary of the tested SNR when $\alpha = 0.95$.

TABLE 2. The number of tested SNR values that fall above the predicted lower boundary for different moving window sizes.

Spacing distance	W_1 =5 W_2 =30	W_1 =10 W_2 =30	W_1 =20 W_2 =30	W_1 =60 W_2 =30	W_1 =10 W_2 =20	W_1 =10 W_2 =40	W_1 =10 W_2 =60
10m	488	488	489	480	487	486	480
50m	490	491	490	480	492	490	479
90m	491	492	490	478	490	492	478

Besides, the shorter moving window size will affect the accuracy of the mean and the variance of the SNR. However, the longer moving window size will make the computed mean and variance not sensitive to the dynamic change. Therefore we have to balance the computation error and sensibility to dynamical change. Table 2 summarizes the number of tested SNR values that fall above the predicted lower boundary for different moving window sizes, the larger the number, the better. Based on the comprehensive analysis of various prediction results at different spacing distances, we choose $W_1 = 10$ and $W_2 = 30$ as the optimal moving window sizes.

Furthermore, the lower boundary of the tested SNR is presented in Fig.7 when $\alpha = 0.95$, $W_1 = 10$ and $W_2 = 30$. As shown in Fig.7, there is a total of 500 tested SNR

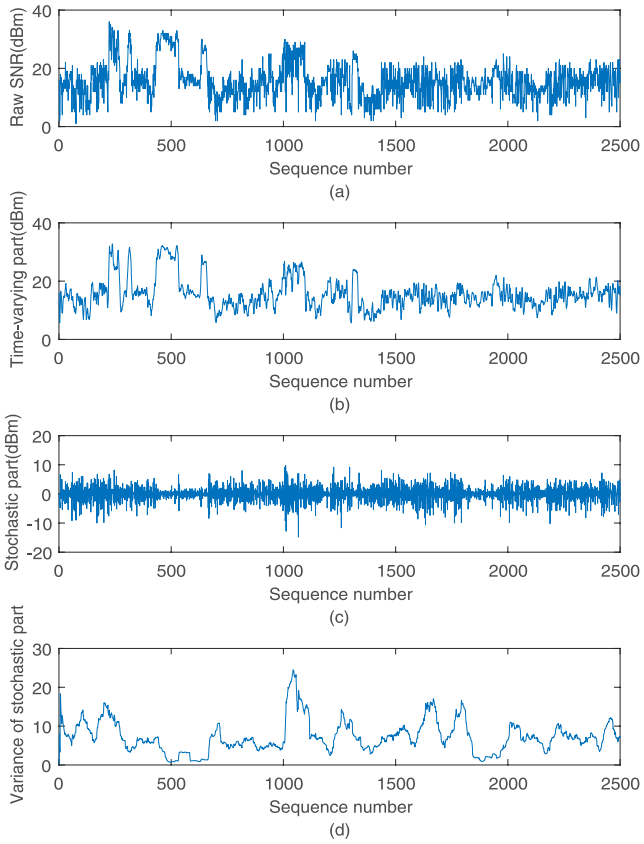

FIGURE 6. In the case of 90m spacing distance: (a) raw SNR sequence, (b) time-varying sequence, (c) stochastic sequence, and (d) variances of stochastic sequence.

data for each WSNs link. Based on the statistic results of the experiments, 488 tested SNR values fall above the predicted lower boundary in Fig.7(a), 491 above in Fig.7(b), and 492 above in Fig.7(c). The results show these data ratios are almost consistent with the specified probability-guaranteed level of 0.95. Therefore, the conclusion can be obviously obtained that the proposed RVFL-LQP algorithm can produce an accurate prediction of the probability-guaranteed interval boundary of link quality.

C. COMPARISON RESULTS AND DISCUSSION

In this section, we carry out a comparative study on the link quality prediction algorithms, including the Expert-Prediction-based LQP algorithm (Expert-Prediction) [39], the XCoPred algorithm [40], the State-Space-based LQP algorithm (State-Space) [41], and our RVFL-LQP algorithm. Different methods are employed as independent forecasting tools to predict the link quality data that collected from the power substation. Furthermore, we compare four different link quality prediction algorithms for those three WSNs link (spacing distance are 10m, 50m and 90m, respectively).

Based on these results shown in Fig.8, Fig.9 and Fig.10, it can be clearly known that: (1) Even the Expert-Prediction, XCoPred, and State-Space algorithms try to predict the exact

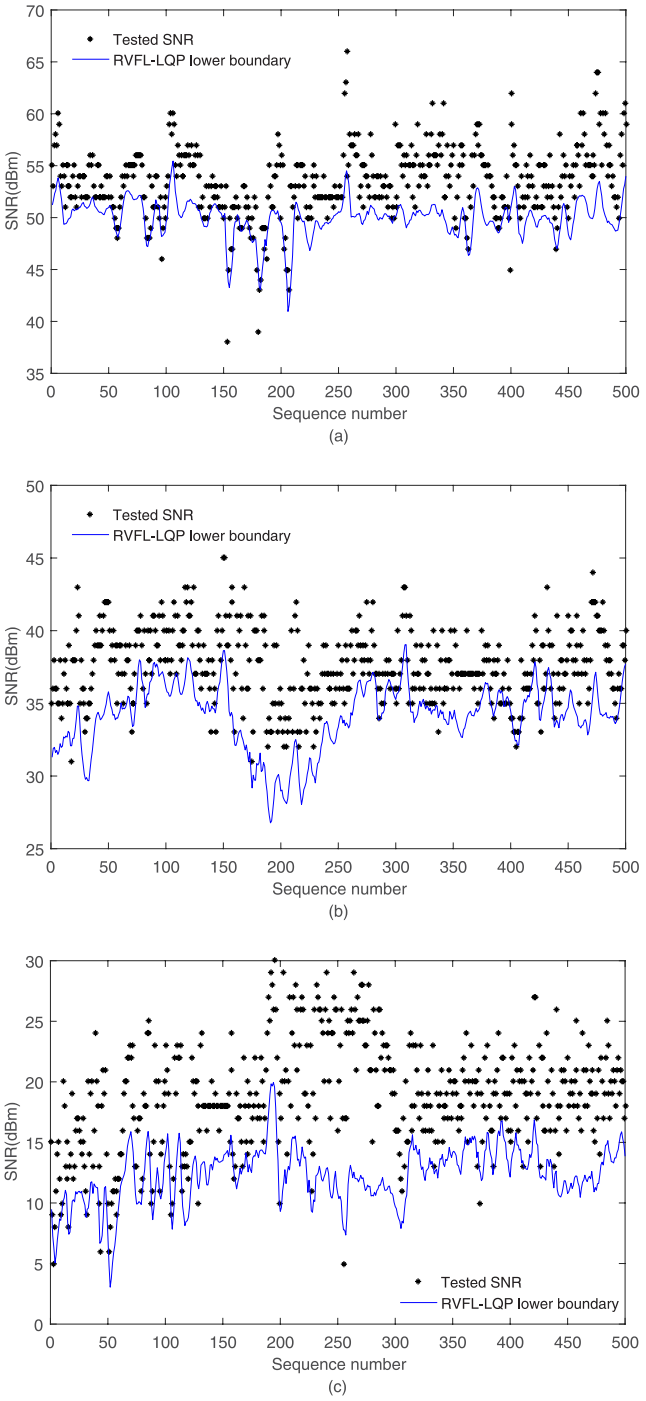

FIGURE 7. The probability-guaranteed interval boundary of the tested SNR: (a) for the 10m spacing distance, (b) for the 50m spacing distance, and (c) for the 90m spacing distance.

value of link quality, however, the stochastic feature makes them deviate the actual value. (2) Our method could give an accurate lower boundary of link quality. Almost all the tested SNR values and prediction results of the Expert-Prediction, XCoPred, State-Space algorithms are above the lower boundary. Therefore our RVFL-LQP algorithm considers the link quality under worst case and helps to determinate the link is good or not.

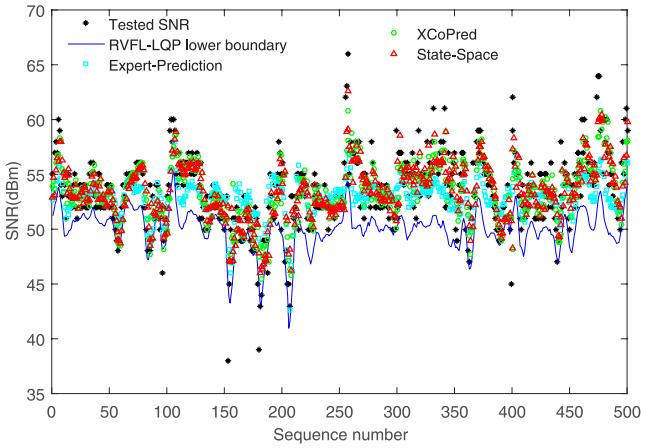

FIGURE 8. Tested SNR data and prediction results of the RVFL-LQP, Expert-Prediction, XCoPred and State-Space algorithms for the 10m spacing distance.

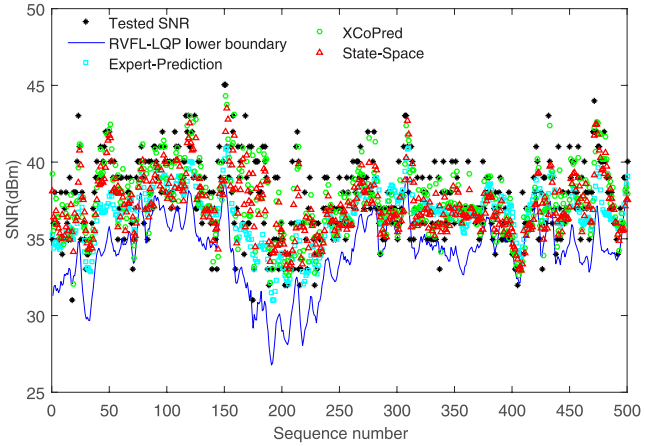

FIGURE 9. Tested SNR data and prediction results of the RVFL-LQP, Expert-Prediction, XCoPred and State-Space algorithms for the 50m spacing distance.

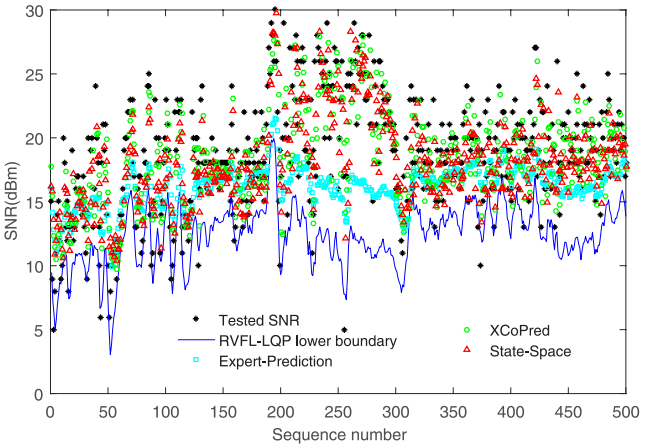

FIGURE 10. Tested SNR data and prediction results of the RVFL-LQP, Expert-Prediction, XCoPred and State-Space algorithms for the 90m spacing distance.

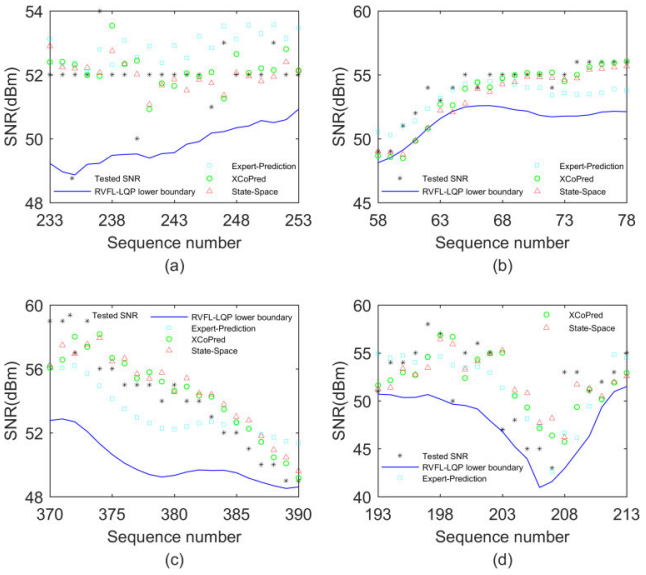

FIGURE 11. Zoomed-in views of the link quality in the case of 10m spacing distance: (a) the steady state, (b) the rising state, (c) the falling state, and (d) the dispersed state.

To further compare four algorithms, we categorize the state of the link quality into the steady state (the SNR remains stable), the rising state (the SNR increases stable), the falling state (the SNR decreases stable), and the dispersed state (the SNR fluctuates relatively large). Fig.11, Fig.12 and Fig.13 show the partial zoom-in views of Fig.8, Fig.9 and Fig.10 respectively.

In the case of a link with 10m spacing distance, combining Fig.11, we can analyze it in detail. When the link quality is in the steady state as depicted in Fig.11(a) (sequence number is between 233 and 253 in Fig.8), the Expert-Prediction, XCoPred and State-Space algorithms all perform well, and the average prediction errors of these algorithms are all less than 1dBm. When the link quality is in the rising state as depicted in Fig.11(b) (sequence number is between 58 and 78 in Fig.8), or in the falling state as depicted in Fig.11(c) (sequence number is between 370 and 390 in Fig.8), the XCoPred algorithm performs best, and the Expert-Prediction algorithm performs worst. When the link quality is in the dispersed state as depicted in Fig.11(d) (sequence number is between 193 and 213 in Fig.8), the average prediction errors of three algorithms above are worse, all within the range of 2.5 to 2.9 dBm.

In the case of a link with 50m spacing distance, combining Fig.12, we can analyze it in detail. When the link quality is in the steady state as depicted in Fig.12(a) (sequence number is between 353 and 373 in Fig.9), the Expert-Prediction, XCoPred, and State-Space algorithms all perform well. When the link quality is in the rising state as depicted in Fig.12(b) (sequence number is between 30 and 50 in Fig.9), the average prediction error of the XCoPred algorithm is lowest (merely 0.9412dBm), and the State-Space algorithm has lower average prediction error than the Expert-Prediction algorithm. When the link quality is in the falling state as depicted

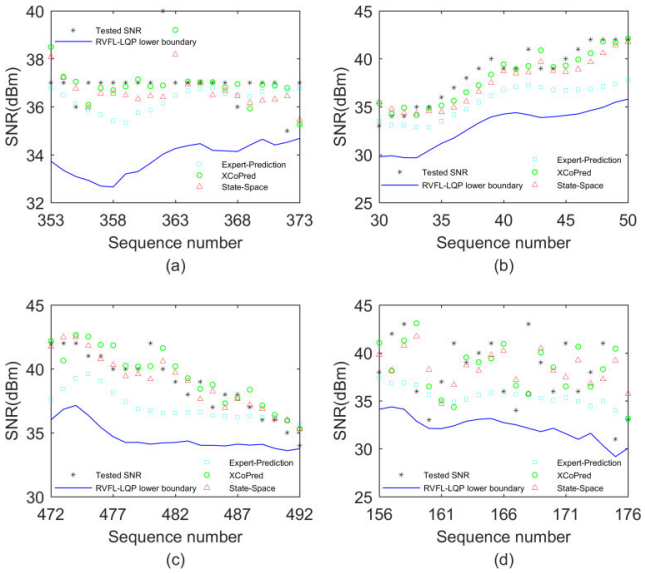

FIGURE 12. Zoomed-in views of the link quality in the case of 50m spacing distance: (a) the steady state, (b) the rising state, (c) the falling state, and (d) the dispersed state.

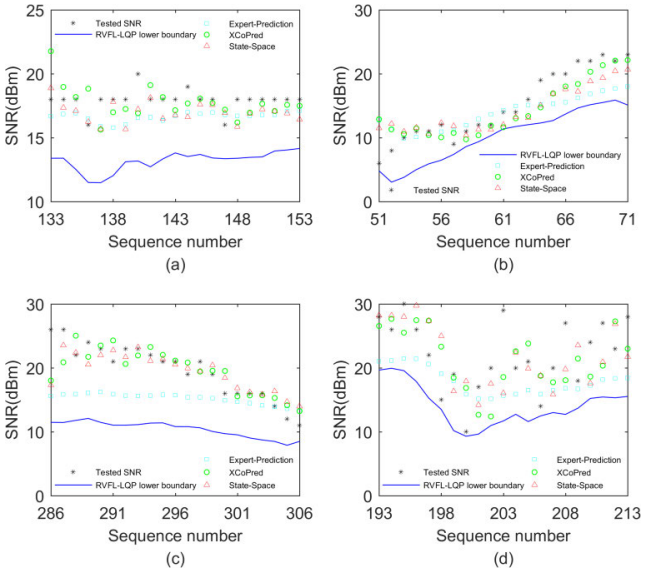

FIGURE 13. Zoomed-in views of the link quality in the case of 90m spacing distance: (a) the steady state, (b) the rising state, (c) the falling state, and (d) the dispersed state.

in Fig.12(c) (sequence number is between 472 and 492 in Fig.9), the State-Space algorithm has lower average prediction error than the Expert-Prediction and XCoPred algorithms. But when the link quality is in the dispersed state as depicted in Fig.12(d) (sequence number is between 156 and 176 in Fig.9), the average prediction errors of the three algorithms are all slightly larger, approximating to 3.4 dBm.

From Fig.13, the same analysis can be made for a link with 90m spacing distance as follows: when the link quality is in the steady state as depicted in Fig.13(a) (sequence number is between 133 and 153 in Fig.10), the State-Space algorithm has lower average prediction error than the Expert-Prediction and XCoPred algorithms. When the link quality is in the rising state as depicted in Fig.13(b) (sequence number is between 51 and 71 in Fig.10), the XCoPred algorithm has lower average prediction error than the Expert-Prediction and State-Space algorithms. When the link quality is in the falling state as depicted in Fig.13(c) (sequence number is between 286 and 306 in Fig.10), the State-Space algorithm performs better than the XCoPred algorithm, and in the meanwhile, the XCoPred algorithm performs better than the Expert-Prediction algorithm. Moreover, when the link quality is in the dispersed state as depicted in Fig.13(d) (sequence number is between 193 and 213 in Fig.10), although the XCoPred algorithm has the best performance, the Expert-Prediction is the worst, the average prediction errors of three algorithms are all still large. With the low accuracy, the maximum average prediction error value even exceeds 5.3dBm. These results show that the prediction results of these three algorithms are not stable.

According to the relationship between SNR and PRR in equation (1), it can be deduced that as the SNR increases, the PRR increases. That is to say, if the tested value is above the prediction result, when the prediction result satisfies the communication requirements, the tested value can also be guaranteed to satisfy the communication requirements. If the tested value is below the prediction result, even if the prediction error is small, it is impossible to guarantee whether the tested value satisfies the communication requirements. We use the index validity of the prediction results to describe the proportion of the tested values above the prediction results.

Table 3-5 summarize the validity of prediction results of Expert-Prediction, XCoPred, State-Space and our RVFL-LQP algorithms in different situations. It can be seen from the statistical results that the tested values are randomly above or below the prediction results in the Expert-Prediction,

TABLE 3. The validity of link quality prediction results for the 10m spacing distance.

Method	Steady state	Rising state	Falling state	Dispersed state	Overall state
Expect-Prediction	4%	76%	67%	57%	56%
XCoPred	38%	76%	19%	62%	49%
State-Space	47%	90%	24%	62%	49%
RVFL-LQP	100%	100%	100%	100%	97%

TABLE 4. The validity of link quality prediction results for the 50m spacing distance.

Method	Steady state	Rising state	Falling state	Dispersed state	Overall state
Expect-Prediction	86%	95%	81%	81%	67%
XCoPred	52%	67%	24%	48%	52%
State-Space	71%	81%	38%	52%	59%
RVFL-LQP	100%	100%	100%	100%	98%

TABLE 5. The validity of link quality prediction results for the 90m spacing distance.

Method	Steady state	Rising state	Falling state	Dispersed state	Overall state
Expect-Prediction	90%	62%	90%	86%	76%
XCoPred	62%	71%	43%	52%	55%
State-Space	80%	71%	43%	52%	57%
RVFL-LQP	100%	100%	100%	100%	98%

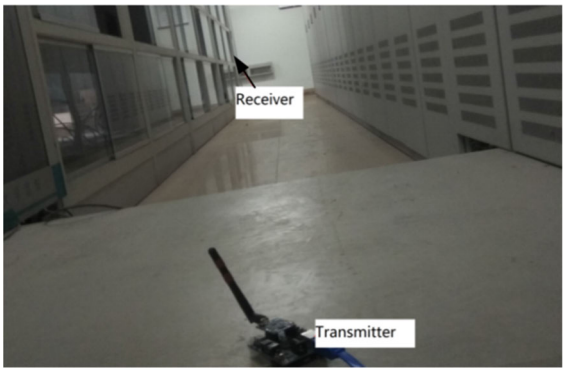

FIGURE 14. The experiment environment of indoor substation.

XCoPred and State-Space algorithms, and the validity of prediction results are unstable. However, the validity of the prediction results of our RVFL-LQP algorithm is always the highest, even up to 100%. In our algorithm, according to the prediction results, the tested value can be guaranteed to satisfy the communication requirements with the maximum probability.

In power systems and other industrial fields, when link quality information is needed to solve routing decisions in data communication, the overall validity of link quality prediction results is more important than its accuracy.

Apparently, from the above analysis, the conclusion of our observations are as follows:

(1) Due to the strong randomness of link quality, the Expert-Prediction, XCoPred, and State-Space algorithms present different prediction results in different situations, and their prediction results are unstable. In general, the stronger the fluctuation is, the more unstable the results are.

(2) The lower boundary predicted by our RVFL-LQP algorithm can adaptively vary with the fluctuations of tested SNR values, and it has high validity. Besides, almost all the tested SNR values fall above the lower boundary, which verified that the proposed RVFL-LQP algorithm can provide an accurate and trustworthy prediction of the probability-guaranteed interval boundary.

Therefore, we can conclude that our algorithm is more valid and stable than other LQP algorithms above.

VI. APPLICATION EXAMPLE

To illuminate the proposed RVFL-LQP algorithm for real-world application in an industrial environment, we predict

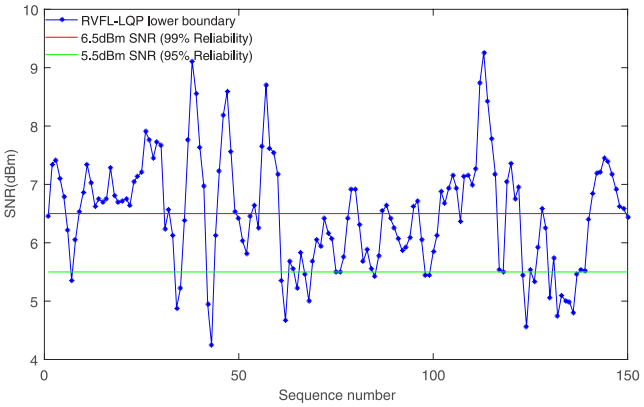

FIGURE 15. The results of application example.

the SNRs for a wireless link at an indoor substation. The experiment environment is shown in Fig.14, one WSNs node is playing as the transmitter and the other one is the receiver, and the transmitter is connected to the PC for collecting the link quality metric (SNR). Based on the collected data, we carry out the RVFL network on the PC online to predict the link quality.

We first performed the simple mathematical operation through equation (6)-(8) to decompose SNR. Then we use the RVFL network to establish the prediction model by equation (10)-(13). The RVFL randomly initializes all weights and biases between the input layer and hidden layer nodes, and the equation (12) is just to obtain the output weights. Then we use equation (13) to calculate the outputs. For the RVFL network, we chose the number of input layer nodes $N_I = 2 \cdot m = 16$, the number of output layer nodes $N_O = 2$, and the optimal number of hidden layer nodes $N_H = 33$. We do only 1154 simple mathematical operations. Finally, we obtain the probability-guaranteed prediction of lower boundary through equation (14)-(15). The whole process is done by basic mathematical operations.

The prediction results are expressed by the blue curve in the Fig.15. In addition, we substitute the PRR requirement of 99% and 95% into (1). Then, we get the corresponding requirement of SNR is 6.5 dBm and 5.5 dBm respectively. In the experiment, the link is randomly obstructed.

As shown in Fig.15, there are 150 predictions of the lower boundary by our RVFL-LQP method. If the prediction value of SNR is above the red line, which means the transmission reliability is higher than 99%. If the prediction value of SNR is between the red line and the green line, which means the transmission reliability is higher than 95% but lower than 99%. Otherwise, the transmission reliability is lower than 95%.

Therefore, we can use the above results to decide whether this link is reliable enough for transmitting the packets of different smart grid applications according to the reliability requirements as in Table 1.

VII. CONCLUSION

In this paper, by analyzing the log-normal path-loss model and using the decomposition method, the SNR time sequence in the wireless link is decomposed into two different parts due to the time-varying and stochastic characteristics. The RVFL method is used to predict the two parts separately, and the probability-guaranteed interval boundary of the communication link quality is derived based on the prediction results. The experiment results show that the lower boundary of link quality can accurately reflect the changing of link quality, and it is more valid than the existing LQP algorithms. In addition, we also illuminate how to apply the RVFL-LQP to provide a reliability prediction in WSNs for smart grid applications by real-world experiment.

Furthermore, we investigate the performance of complex network [42]–[44], we also look forward to further study the following topics:

(1) In consideration of link weight, the reliability prediction of multi-hop wireless links in the network.
(2) Apply the prediction results to the optimal control of smart grid communication to further ensure reliability.

REFERENCES

[1] S. Rekik, N. Baccour, M. Jmaiel, and K. Drira, "Wireless sensor network based smart grid communications: Challenges, protocol optimizations, and validation platforms," *Wireless Pers. Commun.*, vol. 95, no. 4, pp. 4025–4047, Aug. 2017.
[2] S. Kurt, H. U. Yildiz, M. Yigit, B. Tavli, and V. C. Gungor, "Packet size optimization in wireless sensor networks for smart grid applications," *IEEE Trans. Ind. Electron.*, vol. 64, no. 3, pp. 2392–2401, Mar. 2017.
[3] D. He, S. Chan, and M. Guizani, "Cyber security analysis and protection of wireless sensor networks for smart grid monitoring," *IEEE Wireless Commun.*, vol. 24, no. 6, pp. 98–103, Dec. 2017.
[4] H. Hu, Z. Liu, and J. P. An, "Mining mobile intelligence for wireless systems: A deep neural network approach," *IEEE Comput. Intell. Mag.*, to be published.
[5] Z. Liu, T. Tsuda, H. Watanabe, S. Ryuo, and N. Iwasawa, "Data driven cyber-physical system for landslide detection," *Mobile Netw. Appl.*, vol. 24, no. 3, pp. 991–1002, Jun. 2019.
[6] M. Yigit, V. C. Gungor, E. Fadel, L. Nassef, N. Akkari, and I. F. Akyildiz, "Channel-aware routing and priority-aware multi-channel scheduling for WSN-based smart grid applications," *J. Netw. Comput. Appl.*, vol. 71, pp. 50–58, Aug. 2016.
[7] R. C. Vara, J. Prieto, and J. M. Corchado, "How blockchain could improve fraud detection in power distribution grid," in *Proc. Int. Conf. Soft Comput. Mod. Ind. Environ. Appl.*, 2018, pp. 67–76.
[8] P.-Y. Kong, C.-W. Liu, and J.-A. Jiang, "Cost-efficient placement of communication connections for transmission line monitoring," *IEEE Trans. Ind. Electron.*, vol. 64, no. 5, pp. 4058–4067, May 2017.
[9] S. Shao, S. Guo, and X. Qiu, "Distributed fault detection based on credibility and cooperation for WSNs in smart grids," *Sensors*, vol. 17, no. 5, p. 983, Apr. 2017.
[10] U. Bodin and K. Wolosz, "Proportional throughput differentiationwith cognitive load-control on WSN channels," *EURASIP J. Wireless Commun. Netw.*, vol. 2015, Jul. 2015, Art. no. 186.
[11] N. Kilic and V. C. Gungor, "Analysis of low power wireless links in smart grid environments," *Comput. Netw.*, vol. 57, no. 5, pp. 1192–1203, Apr. 2013.
[12] J. Shu, S. Liu, L. L. Liu, and X. L. Gu, "Link quality prediction for WSNs based on dynamic Bayesian networks," *Adv. Eng. Sci.*, vol. 49, no. 2, pp. 152–159, Mar. 2017.
[13] X. Zhou, X. Ji, Y.-C. Chen, X. Li, and W. Xu, "LESS: Link estimation with sparse sampling in intertidal WSNs," *Sensors*, vol. 18, no. 3, p. 747, Mar. 2018.
[14] F. Qin, Q. Zhang, W. Zhang, Y. Yang, J. Ding, and X. Dai, "Link quality estimation in industrial temporal fading channel with augmented Kalman filter," *IEEE Trans. Ind. Informat.*, vol. 15, no. 4, pp. 1936–1946, Apr. 2019.
[15] G. Cerar, M. Mohorcic, T. Gale, and C. Fortuna, "Analysis of machine learning for link quality estimation," Feb. 2019, *arXiv:1812.08856*. [Online]. Available: https://arxiv.org/abs/1812.08856
[16] C. Renner, S. Ernst, C. Weyer, and V. Turau, "Prediction accuracy of link-quality estimators," in *Proc. Eur. Conf. Wireless Sensor Netw.*, Bonn, Germany, Feb. 2011.
[17] N. Reijers, G. Halkes, and K. Langendoen, "Link layer measurements in sensor networks," in *Proc. IEEE Int. Conf. Mobile Ad-Hoc Sensor Syst.*, Fort Lauderdale, FL, USA, Feb. 2005, pp. 224–234.
[18] Y. Chen and A. Terzis, "On the mechanisms and effects of calibrating RSSI measurements for 802.15.4 radios," in *Proc. Eur. Conf. Wireless Sensor Netw.*, Berlin, Germany, Feb. 2010, pp. 256–271.
[19] K. Srinivasan, P. Dutta, A. Tavakoli, and P. Levis, "An empirical study of low-power wireless," *ACM Trans. Sensor Netw.*, vol. 6, no. 2, pp. 1–49, Feb. 2010.
[20] M. Senel, K. Chintalapudi, D. Lal, A. Keshavarzian, and E. J. Coyle, "A Kalman filter based link quality estimation scheme for wireless sensor networks," in *Proc. IEEE Global Telecommun. Conf. (GLOBECOM)*, Nov. 2007, pp. 875–880.
[21] A. Woo, T. Tong, and D. Culler, "Taming the underlying challenges of reliable multihop routing in sensor networks," in *Proc. 1st Int. Conf. Embedded Netw. Sensor Syst. (SenSys)*, 2003, pp. 14–27.
[22] K. Srinivasan, M. A. Kazandjieva, S. Agarwal, and P. Levis, "The beta-factor: Measuring wireless link burstiness," in *Proc. ACM Sensor Syst.*, 2008, pp. 29–42.
[23] P. Moinzadeh, K. Mechitov, and G. Agha, "Link quality estimation for data-intensive sensor network applications," *Comput. Sci. Res. Technol. Rep.*, Sept. 2011. [Online]. Available: http://hdl.handle.net/2142/26515
[24] Y. Wang, M. Martonosi, and L.-S. Peh, "Predicting link quality using supervised learning in wireless sensor networks," *Mobile Comput. Commun. Rev.*, vol. 11, no. 3, p. 71, Jul. 2007.
[25] D. S. J. De Couto, D. Aguayo, J. Bicket, and R. Morris, "A high-throughput path metric for multi-hop wireless routing," *Wireless Netw.*, vol. 11, no. 4, pp. 419–434, Jul. 2005.
[26] C. A. Boano, M. A. Zuniga, T. Voigt, A. Willig, and K. Romer, "The triangle metric: Fast link quality estimation for mobile wireless sensor networks," in *Proc. 19th Int. Conf. Comput. Commun. Netw.*, Zürich, Switzerland, 2010, pp. 1–7.
[27] N. Baccour, A. Koubaa, H. Youssef, M. B. Jamaa, D. Rosario, M. Alves, and L. B. Becker, "F-LQE: A fuzzy link quality estimator for wireless sensor networks," in *Proc. Eur. Conf. Wireless Sensor Netw.*, Berlin, Germany, 2010, pp. 240–255.
[28] T. Jayasri and M. Hemalatha, "Link quality estimation for adaptive data streaming in WSN," *Wireless Pers. Commun.*, vol. 94, no. 3, pp. 1543–1562, Jun. 2017.
[29] D. Liu, Z. Cao, M. Hou, and Y. Zhang, "Frame counter: Achieving accurate and real-time link estimation for low power wireless sensor networks," *ACM Trans. Netw.*, vol. 25, no. 4, pp. 2096–2109, 2017.
[30] V. C. Gungor, D. Sahin, T. Kocak, S. Ergut, C. Buccella, C. Cecati, and G. P. Hancke, "A survey on smart grid potential applications and communication requirements," *IEEE Trans. Ind. Informat.*, vol. 9, no. 1, pp. 28–42, Feb. 2013.
[31] M. Z. Zamalloa and B. Krishnamachari, "An analysis of unreliability and asymmetry in low-power wireless links," *ACM Trans. Sensor Netw.*, vol. 3, no. 2, p. 7, Jun. 2007.
[32] K. K. Shang, W. S. Yan, and M. Small, "Evolving networks—Using past structure to predict the future," *Phys. A, Stat. Mech. Appl.*, vol. 455, pp. 120–135, Aug. 2016.
[33] K.-K. Shang, T.-C. Li, M. Small, D. Burton, and Y. Wang, "Link prediction for tree-like networks," *Chaos*, vol. 29, no. 6, Jun. 2019, Art. no. 061103, doi: 10.1063/1.5107440.
[34] W. Sun, X. Yuan, J. Wang, Q. Li, L. Chen, and D. Mu, "End-to-end data delivery reliability model for estimating and optimizing the link quality of industrial WSNs," *IEEE Trans. Automat. Sci. Eng.*, vol. 15, no. 3, pp. 1127–1137, Jul. 2018.
[35] J. Xu, W. Liu, F. Lang, Y. Zhang, and C. Wang, "Distance measurement model based on RSSI in WSN," *Wireless Sensor Netw.*, vol. 2, no. 8, pp. 606–611, 2010.
[36] Z. Li and Q. Liang, "Performance analysis of multiuser selection scheme in dynamic home area networks for smart grid communications," *IEEE Trans. Smart Grid*, vol. 4, no. 1, pp. 13–20, Mar. 2013.
[37] V. C. Gungor, B. Lu, and G. P. Hancke, "Opportunities and challenges of wireless sensor networks in smart grid," *IEEE Trans. Ind. Electron.*, vol. 57, no. 10, pp. 3557–3564, Oct. 2010.
[38] D. Mu, L. Chen, W. Sun, J. Wang, and Q. Li, "A radio link reliability prediction model for wireless sensor networks," *Int. J. Sensor Netw.*, vol. 27, no. 4, pp. 215–226, 2017.

[39] D. Marinca and P. Minet, "On-line learning and prediction of link quality in wireless sensor networks," in *Proc. IEEE Global Commun. Conf.*, Dec. 2014, pp. 1245–1251.
[40] K. Farkas, T. Hossmann, F. Legendre, B. Plattner, and S. K. Das, "Link quality prediction in mesh networks," *Comput. Commun.*, vol. 31, no. 8, pp. 1497–1512, May 2008.
[41] X. Ma, J. Liao, S. M. Djouadi, and Q. Cao, "LIPS: Link prediction as a service for data aggregation applications," *Ad Hoc Netw.*, vol. 19, pp. 43–58, Aug. 2014.
[42] L. Lü and T. Zhou, "Link prediction in weighted networks: The role of weak ties," *Europhys. Lett.*, vol. 89, no. 1, Jan. 2010, Art. no. 18001.
[43] K.-K. Shang, M. Small, and W.-S. Yan, "Link direction for link prediction," *Phys. A, Stat. Mech. Appl.*, vol. 469, pp. 767–776, Mar. 2017.
[44] K.-K. Shang, M. Small, X.-K. Xu, and W.-S. Yan, "The role of direct links for link prediction in evolving networks," *Europhys. Lett.*, vol. 117, no. 2, Jan. 2017, Art. no. 28002.

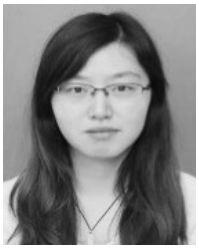

XUE XUE received the B.S. degree in automation from Anhui Polytechnic University, China, in 2011, and the M.S. degree in detection technology and automatic equipment from the Hefei University of Technology, in 2014. She is currently pursuing the Ph.D. degree in electrical engineering with the Hefei University of Technology. Her main research interests include smart grid, wireless sensor network, and intelligent information processing.

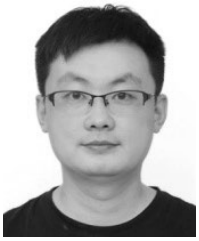

WEI SUN (Member, IEEE) received the B.S. degree in automation, the M.S. degree in detection technology and automatic equipment, and the Ph.D. degree in electrical engineering from the Hefei University of Technology, China, in 2004, 2007, and 2012, respectively. He is currently an Associate Professor with the Hefei University of Technology. His research interests include wireless sensor networks, networked control systems, and smart grid.

JIANPING WANG received the B.S. and M.S. degrees from the Hefei University of Technology, China, in 1978 and 1987, respectively. He is currently a Professor and a Doctoral Supervisor with the Hefei University of Technology. His main research interests include intelligent system and electrical control technology, wireless sensor network, and pattern recognition.

QIYUE LI (Member, IEEE) received the B.S. degree in electronic engineering from Wuhan University, China, in 2003, and the Ph.D. degree in communication and information system from the University of Science and Technology, China. From 2008 to 2011, he was a Postdoctoral Research with the School of Computer Science and Technology, University of Science and Technology. He is currently an Associate Professor with the Hefei University of Technology, China. His research interests include wireless sensor networks and indoor localization using wireless networks.

GUOJUN LUO is currently an Associate Professor with the Hefei University of Technology, China. His research interests include computer control, computer networks, and data communication.

KEPING YU (Member, IEEE) received the M.S. and Ph.D. degrees from the Graduate School of Global Information and Telecommunication Studies, Waseda University, Tokyo, Japan, in 2012 and 2016, respectively.

He is currently a Junior Researcher with the Global Information and Telecommunication Institute, Waseda University. His research interests include smart grids, information-centric networking, the Internet of Things, blockchain, and information security. He has served as a TPC Member of the IEEE VTC2019-Spring, ITU Kaleidoscope 2019, IEEE HotICN 2019, IEEE ICCC 2019, IEEE WPMC 2019, EEI2019, ICITVE2019, IEEE CCNC 2020, and IEEE WCNC 2020. He is also an Editor of the IEEE Open Journal of Vehicular Technology (OJVT).